A New Multi-Axial Creep-Damage Model and Its Application in Creep Crack Growth Predictions

Jian-Feng Wen[1] and Shan-Tung Tu[2]

Key Laboratory of Pressure Systems and Safety (Ministry of Education), School of Mechanical and Power Engineering, East China University of Science and Technology, Shanghai 200237, PR China

[1]Email: jianfengwen@gmail.com
[2]Corresponding author, Email: sttu@ecust.edu.cn

ABSTRACT. *This paper presents a creep constitutive reasonably reflecting the influence of stress triaxiality on creep deformation and a creep cavity growth model appropriately describing the effect of stress biaxiality on the multi-axial creep ductility. Three-dimensional finite element analyses are performed to simulate the creep growth behaviors of a single crack in thumbnail crack specimens and multiple cracks in a tensioned plate at high temperature, respectively. Numerical results show the proposed creep-damage model is proved to be of excellent predictive capability.*

INTRODUCTION

It is no exaggeration to say that crack-like defects inevitably exist in most components and the assessment of them is very crucial since it indicates whether they are safe enough or not. Owing to a crack revealed on an engine blade, US military recently grounded all F-35 fighter jets before the investigation being complete [1]. Intuitively, we might expect a robust and time-saving assessment approach such as numerical simulation to be adopted.

Undoubtedly, an appropriate creep-damage model is necessary for the reliable simulation of crack growth with creep regime. Although significant progress has been made in the continuum damage mechanics (CDM) model to simulate creep failure [2-8], some obstacles need to be overcome. One of the major difficulties is how to simplify the increasingly complicated model without the loss of reality and accuracy.

In this work, a creep constitutive combined with a modified creep cavity growth

model under multi-axial stresses is proposed. Furthermore, its applicability in creep crack growth prediction is demonstrated.

CREEP-DAMAGE MODEL

The first CDM model, which was envisaged in Kachanov and Rabotnov's work [2, 3] in 1960s, was reported to give significantly mesh-dependent results [4]. This led Liu and Murakami to suggest an alternative one in which the ill-natured stress sensitivity was avoided. However, the influence of stress triaxiality has not been reasonably considered and the over-complicated model needs to be simplified.

Using a modified creep ductility exhaustion approach, the authors [9] presented a creep-damage model, which does not require the calibration of parameters in the damage calculation, to simulate creep failure. The proposed model is as follows:

$$\dot{\varepsilon}_{ij}^{c} = \frac{3}{2} A \sigma_e^{n-1} s_{ij} \left[1 + \beta \left(\frac{\sigma_1}{\sigma_e} \right)^2 \right]^{\frac{n+1}{2}}, \tag{1}$$

and

$$\dot{\omega} = \frac{\dot{\varepsilon}^{c}}{\varepsilon_f^{*}}, \tag{2}$$

where A and n are material constants. ε_{ij}^{c}, s_{ij}, σ_e and σ_1 are the creep strain tensor, deviatoric stress tensor, equivalent stress and maximum principle stress, respectively. ω, $\dot{\varepsilon}^{c}$ and ε_f^{*} denote the damage variable, creep strain rate and multi-axial creep failure strain, respectively. β is a function of n and ω, of which the expression is given in Refs. [9].

Fig. 1 shows the relation between creep rate enhancement and stress triaxiality for ω=0.5391. The enhancement factor, e, is defined as the ratio of creep strain rate with damage to that without damage. It is clear from Fig. 1 that when stress triaxiality is more than one, the enhancement factors predicted by Liu-Murakami model appear not to match the cell model calculations of Sester et al. [10], while the proposed model can better reflect the effect of stress state on creep deformation.

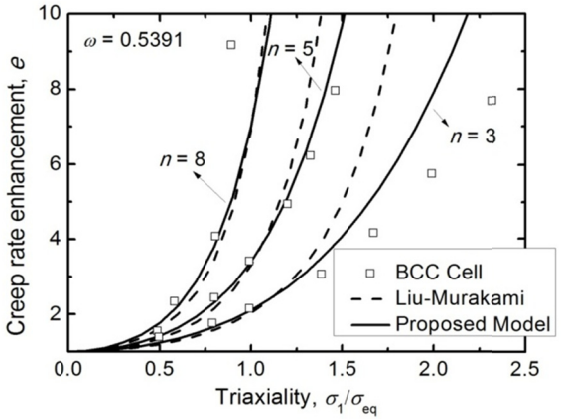

Figure 1. Relation between creep rate enhancement and stress triaxiality

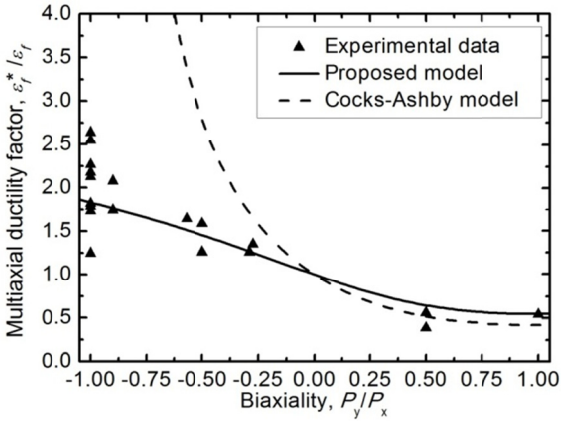

Fig. 2. Effect of biaxiality on the creep ductility

It is known that the creep ductility also significantly depends on the stress state. In this work, a modified creep cavity growth model is employed to quantify the multi-axial stress effect on creep ductility:

$$\frac{\varepsilon_f^*}{\varepsilon_f} = \exp\left[\frac{2}{3}\left(\frac{n-0.5}{n+0.5}\right)\right] \Big/ \exp\left[2\left(\frac{n-0.5}{n+0.5}\right)\frac{\sigma_m}{\sigma_e}\right], \tag{3}$$

where ε_f is the uniaxial creep failure strain and σ_m is the hydrostatic stress.

Fig. 2 depicts the effect of biaxiality on the creep ductility predicted by the widely-used Cocks-Ashby model [11] and the proposed model, in which P_y/P_x denotes the biaxial stress ratio. The experimental ductility data from literature [12] for 316 stainless steel tested at 600 ºC and 593 ºC are also duplicated in Fig. 2. One can find that Cocks-Ashby model is not conservative completely for $P_y/P_x < 0$, while multi-axial ductility factor predicted by the proposed model is consistent with the experimental data for the whole range of biaxial stress ratio and therefore, can be considered to be a good approximation.

FINITE ELEMENT TECHNIQUE

On the basis of the creep-damage model described in the previous section, Finite Element (FE) modeling is performed using the codes ABAQUS with the elastic-plastic-creep properties. The true stress-strain data beyond the yield point is used as input to FE analysis and a Mises flow rule with isotropic strain hardening is employed. Eq. 1 is implemented into the ABAQUS user subroutine, CREEP, to define

the time-dependent and damage-coupled creep behavior. Also, Eqs 2 and 3 are embedded in CREEP to determine the damage accumulation. When creep damage variable at a Gauss point is accumulated to 0.99, all the stress components are sharply reduced to a small plateau and thus crack growth can be characterized by a completely damaged element zone ahead of the initial crack tip. In order to embody this failure simulation technique, another user subroutine, USDFLD, is employed.

APPLICATION IN CREEP CRACK GROWTH

In this section we demonstrate the applicability of the proposed model implemented with the numerical technique in creep crack growth prediction in two cases.

Predictions of creep crack growth in thumbnail crack specimens

Three-dimensional creep damage analyses are performed to simulate the creep crack growth in thumbnail crack specimens, of which the geometry is shown in Fig. 3. The specimens under static loads of tension were tested at 600 ºC by Hyde [13]. Two specimens with extensive creep crack growth are chosen, of which test conditions are summarized in Table 1. The material constants employed in the FE analyses are listed in Table 2 [6, 13, 14]. One quarter of the model consisting of about 10,000 eight-node C3D8R elements is established exploiting the symmetry conditions. The mesh size in the vicinity of the crack front is 200μm.

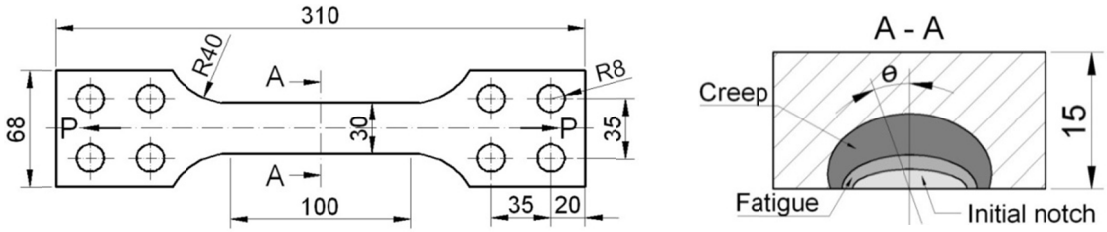

(a) (b)

Figure 3. Geometry of a thumbnail crack specimen: (a) a whole geometry; (b) an enlarged section view on A-A.

Table 1. Test conditions for the thumbnail crack specimens tested at 600 ºC.

Specimen No.	Initial creep crack size (mm)		Load (N)	Test duration (h)
	at $\theta = 0^{o}$	at $\theta = 90^{o}$		
5	2.88	4.33	90800	2760
6	3.50	4.37	90700	1200

Table 2. Material properties of the 316 stainless steel tested at 600ºC.

E (MPa)	ν	A (MPa^{-n}h^{-1})	n	ε_f (%)
148000	0.3	1.47×10^{-29}	10.147	27

Predicted crack profiles using continuum damage mechanics approach are compared with the tested specimen photos [13] in Fig. 4. Obviously, the FE predicted crack fronts match very closely to the experimental results. One can also find that the crack propagates with larger increment at θ = 0º (approximately under plane-strain condition) than that at θ = 90º (approximately under plane-stress condition) due to the constraint effect. Propagation times predicted by the numerical simulation are also in good agreement with the test durations. These encouraging results prove the validity and predictive capability of the proposed creep-damage model presented in Eqs 1 and 2.

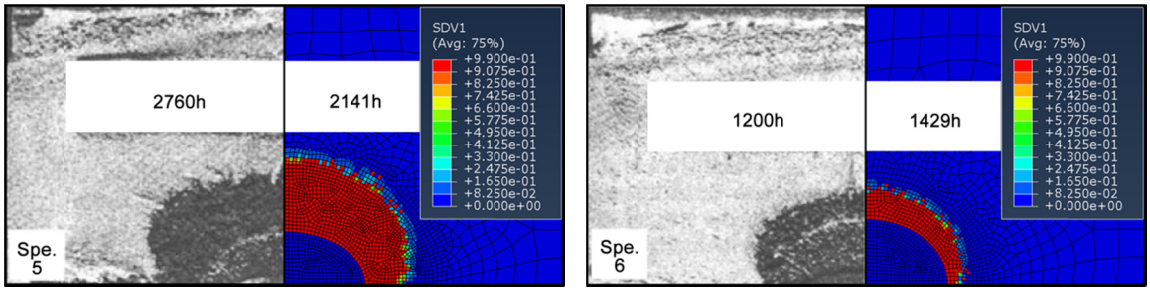

(a) (b)

Figure 4. Comparisons of tested specimen photos with predictions using continuum damage mechanics approach: (a) specimen 5; (b) specimen 6

Predictions of creep growth and coalescence of twin surface cracks in a tensioned plate

Three-dimensional FE analyses are also conducted to simulate the interaction behavior of twin surface cracks in a 316 stainless steel plate at 600 ºC. Fig. 5 shows the geometry of the plate under tension, $\sigma = 201.56$ MPa . The half-length, H, half-width, W, and thickness, t, of the plate are 50 mm, 30 mm and 15 mm respectively. Two pre-cracks is introduced with depth, a = 3.5 mm, and half-length, c = 4.37 mm. The minimum distance, s, between them is selected as 10 mm. Due to the symmetry conditions of geometry and loading, one quarter of the model consisting of about 35,000 eight-node C3D8R elements is built.

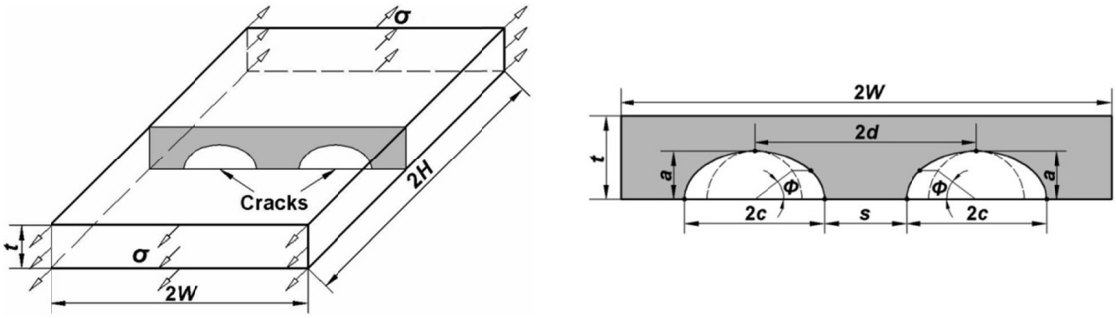

Figure 5. Finite thickness plate containing two semi-elliptical surface cracks under tension.

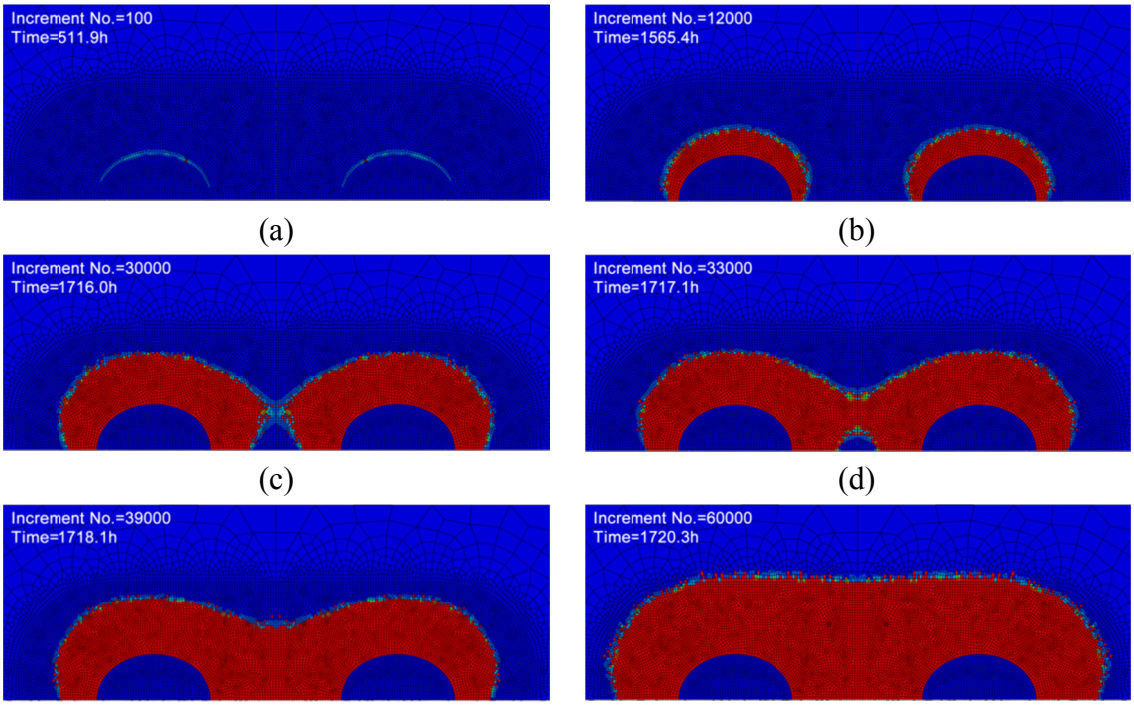

Figure 6. Predicted shape evolution of two identical surface cracks

Predicted shape evolution of the two identical surface cracks is also given. In Fig. 6(a) at 511.9 h, the crack initiation occurs where the stress triaxiality is the highest. It is seen in Fig. 6(b) that the individual crack grows almost independently before the half of the minimum distance between them, $s/2$, is nearly to the initial crack depth, a_0. When the two cracks are close to each other, as shown in Fig. 6(c), much more significant crack propagation is observed in the neighboring zone than in other region. It is natural to think of this as the resulting from the enlarged stress at the reduced remaining ligament. Figs 6(d), (e) and (f) illustrate how crack shape evolves after the contact. When the two

cracks coalesce, dented portions at the contact point are formed by the newly combined crack, with the crack shape deviating from the semi-ellipse pronouncedly. Subsequently, the concave positions of crack front show a relatively high growth rate compared with other sections. Ultimately, the crack shape saturates with the re-entrant section being smooth in a short time.

CONCLUSIONS

Conclusions from this work can be listed below:

(1) The proposed multi-axial creep constitutive can better reflect the effect of stress triaxiality on creep deformation than the widely- used Liu-Murakami model.

(2) The effect of stress biaxiality on the multi-axial creep ductility can be appropriately predicted by the modified creep cavity growth model.

(3) Both of the crack fronts and propagation times of thumbnail crack specimens predicted by using the proposed creep-damage model are in excellent agreement with the experimental results.

(4) The creep growth and coalescence of multiple surface cracks can also be reasonably described in detail by using the proposed model.

ACKNOWLEDGEMENTS

This work is financially supported by National Natural Science Foundation of China (Contract No. 50835003). The authors would also like to thank Prof. T.H. Hyde and Prof. W. Sun at University of Nottingham for the helpful discussion with them.

REFERENCES

1. Garamone, J., (2013), F-35s Grounded as Precaution after Crack Found in Engine Blade, Feb. 22, 2013, http://www.defense.gov/news/newsarticle.aspx?id=119362.
2. Kachanov, L. M., (1958), *Izvestia Akademii Nauk SSSR, Otdelenie Tekhnicheskich Nauk*, **8**, pp. 26-31.
3. Rabotnov, Y. N., (1969), In: *Creep Problems in Structural Members*, North-Holland, Amsterdam.
4. Murakami, S., Liu, Y., and Mizuno, M., (2000), *Comput. Meth. Appl. Mech. Eng.*, **183**, pp. 15-33.
5. Lemaitre, J., and Desmorat, R., (2005), In: *Engineering Damage Mechanics:*

Ductile, Creep, Fatigue and Brittle Failures, Springer-Verlag, Berlin.
6. Hyde, C. J., Hyde, T. H., Sun, W., and Becker, A. A., (2010), *Eng. Fract. Mech.*, **77**, pp. 2385-2402.
7. Yatomi, M., and Tabuchi, M., (2010), *Eng. Fract. Mech.*, **77**, pp. 3043-3052.
8. Oh, C. S., Kim, N. H., Kim, Y. J., Davies, C., Nikbin, K., and Dean, D., (2011), *Eng. Fract. Mech.*, **78**, pp. 2966-2977.
9. Wen, J. F., Tu, S. T., Gao, X. L., and Reddy, J. N., (2013), *Eng. Fract. Mech.*, **98**, pp. 169-184.
10. Sester, M., Mohrmann, R., and Riedel, H., (1997), *ASTM STP*, **1297**, pp. 37-53.
11. Cocks, A. F., and Ashby, M. F., (1980), *Metal Sci.*, **8**, pp. 395-402.
12. Spindler, M. W., (2004), *Fatigue Fract. Eng. Mater. Struct.*, **27**, pp. 273-281.
13. Hyde, T. H., (1988), *High Temp. Technol.*, **6**, pp. 51-61.
14. Smith, S. D., Webster, J. J., and Hyde, T. H., (1988), *Eng. Fract. Mech.*, **30**, pp. 105-116.